applied sciences

MDPI

Article

Equivalent Axial Stiffness of Horizontal Stays

Pietro Croce

Department of Civil and Industrial Engineering, University of Pisa, Largo Lazzarino, 1-56122 Pisa, Italy; p.croce@ing.unipi.it; Tel.: +39-335-534-5611

Received: 18 August 2020; Accepted: 6 September 2020; Published: 9 September 2020

Abstract: Cable-stayed structures are widely employed in several fields of civil, industrial, electrical and ocean engineering. Typical applications are cable-stayed building roofs, bridges, guyed masts, overhead electrical lines, and floating device anchorages. Since the cable behavior is often highly nonlinear, suitable equivalent mechanical cable models are often adopted in analyzing this kind of structures. Usually, like in the classical Dischinger's approach, stays are treated as straight rods offering an equivalent axial tangent stiffness, so that each of them can be substituted with an appropriate equivalent nonlinear spring or truss element. Formulae expressing equivalent stiffness provided by classical methods are satisfactory only when the cable is highly stressed, and therefore its sag is small with respect to its chord; on the contrary, when the cable is slack, they give often contradictory or meaningless results. Aiming to remove that limitation, a more refined approach based on the application of the virtual work principle is discussed. Important products of that original rational criterion are accurate and closed form innovative expressions of the tangent stiffness of the cable, whose field of application is independent on the sag to chord ratio of the cable, as well as on the magnitude of the normal stresses. Referring to some relevant case studies, the results obtained applying these new formulae are critically discussed for cables made of different materials, also in comparison with the approximate expressions provided by simplified methods.

Keywords: stay; cable; equivalent stiffness; Dischinger's modulus; catenary; nonlinear behavior; virtual work principle; cable stayed; overhead lines

1. Introduction

Cable-stayed structures, like cable-stayed building roofs, bridges, extradosed bridges, overhead electrical lines, guyed masts, anchorage of floating devices, cable trusses, etc., are widely used in several engineering fields. From the structural point of view, these structures are extremely appealing; however, since they are often characterized by highly nonlinear behavior, their analysis requires the introduction of refined mechanical models. A very effective simplified mechanical model is commonly considered to simulate the behavior of the stays, where each of them is substituted with a suitable equivalent nonlinear spring or truss element.

In the classical approach, as proposed by Dischinger [1,2] or Ernst [3], the stay is modeled as an equivalent straight bar connecting its ends. The equivalence criterion is that the axial stiffness of the substitutive rod equals the apparent global stiffness of the stay along its chord, i.e., the line connecting its ends.

Assuming that the influences of the bending stiffness of the cable on the deformed configuration is negligible with respect to the axial stiffness of the cable, the traditional treatment of the problem is based on the equilibrium equation of a deformed cable, with horizontal chord, subjected to the self-weight.

Let $\vec{p}$ be the weight of the cable per unit length; since the deformed configuration of the cable belongs to the π plane defined by the two cable ends and by the vector $\vec{p}$ lying on it, classical simplified formulae have been deduced, simulating the cable behavior in terms of an equivalent axial stiffness.

The so-called equivalent modulus can be expressed in form of an equivalent tangent elastic modulus or an equivalent secant elastic modulus. Let a be the length of the cable chord; A_0 the area of the cross section of the cable; E the elastic modulus of the material; $\vec{N}$ the tensile force in the cable, whose horizontal and vertical components are N_0, and N_y, respectively; $\vec{N} = \left(N_0, N_y\right)$, the equivalent elastic modulus of a horizontal stay; $E_{t,eq}(\sigma_0)$, is thus given by the so called Dischinger's formula,

$$E_{t,eq}(\sigma_0) = \frac{d\sigma_0}{d\varepsilon} = \frac{E}{1 + \frac{(\gamma\, a)^2}{12\, \sigma_0^3}\, E} \tag{1}$$

which is widely used for structural design purposes. In Equation (1), σ_0 is the horizontal component of the cable tension, $d\varepsilon$ is the equivalent strain variation in the chord direction and γ is the ratio between the unit weight p and the area A_0, i.e., the specific weight of the cable material. As known, N_0, and σ_0, are independent on the abscissa of the considered section.

Of course, since the problem is governed by geometric nonlinearity only, the material is assumed linear elastic, therefore E is independent on σ_0.

As summarized in the following, Equation (1) was derived by Dischinger [1,2] starting from the expression of the strain variation along the chord direction

$$d\varepsilon = d\varepsilon_e + d\varepsilon^* \tag{2}$$

where $d\varepsilon_e$ is the variation of the elastic strain, and $d\varepsilon^*$ is the apparent variation of the strain.

Following Dischinger, when an inextensible cable, whose length is L, is stretched, the cable configuration changes. If the chord length a increases, the sag and the difference $(L - a)$ reduce and vice versa, i.e., if the chord length a decreases, the sag and the difference $(L - a)$ increase; in any case, this causes the apparent strain variation $d\varepsilon^*$. Obviously, it is

$$d\varepsilon_e = \frac{d\sigma_0}{E},\; d\varepsilon^* = \frac{d\sigma_0}{E^*(\sigma_0)}, \tag{3}$$

being E^* the apparent elastic modulus resulting from the variation of the inextensible cable configuration. From Equations (2) and (3) it follows

$$E_{t,eq}(\sigma_0) = \frac{d\sigma_0}{d\varepsilon} = \frac{d\sigma_0}{d\varepsilon_e + d\varepsilon_f} = \frac{E}{1 + \frac{E}{E^*(\sigma_0)}}, \tag{4}$$

Hypothesizing a parabolic deformed configuration, and assuming the cable sag d much smaller than the chord a, i.e., $d < 0.1\, a$, the length L of an inextensible cable can be approximated by

$$L \cong a + \frac{8\, d^2}{3\, a}. \tag{5}$$

Recalling that the cable sag depends on N_0 through the equilibrium equation,

$$d = \frac{p\, a^2}{8\, N_0}, \tag{6}$$

the contribution to the chord variation due to the modification of the cable configuration induced by $dN_0 \cdot da^*$ can be expressed by

$$da^* = -\frac{d(L-a)}{dN_0} dN_0 \cong -\frac{16\, d}{3\, a} \frac{d}{dN_0}\left(\frac{p\, a^2}{8\, N_0}\right) dN_0 = \frac{p^2\, a^3}{12\, N_0^3} dN_0. \tag{7}$$

Finally, setting $da^* = a\, d\varepsilon_f$ and simplifying, Equation (7) provides

$$\frac{1}{E_f} = \frac{d\varepsilon_f}{d\sigma_0} = \frac{\gamma^2\, a^2}{12\, \sigma_0^3}. \tag{8}$$

Remarking $E_f = E^*(\sigma_0)$, Dischinger deduces thus the equivalent modulus, expressed by Equation (1), simply substituting Equation (8) in Equation (4).

When a large stress variation needs to be taken into account in the cable, it is common practice to consider, rather than the tangent modulus, the equivalent secant elastic modulus, $E_{s,eq}$. Let σ_{01} be the normal stresses at the initial point of the given loading process and σ_{02} the normal stress at the final point of the given loading process; $\Delta\sigma_0 = \sigma_{02} - \sigma_{01}$, $E_{s,eq}$ can be expressed by

$$E_{s,eq} = \frac{\Delta\sigma_0}{\Delta\varepsilon} = \frac{E}{1 + \frac{(\gamma\, a)^2}{24\, \sigma_{01}^3}\, \frac{1+\overline{\sigma}}{\overline{\sigma}^2} E}, \tag{9}$$

where $\overline{\sigma} = \sigma_{02}/\sigma_{01}$.

According to Ernst [3], Equation (9) is obtained using the Dischinger approach and considering the chord length variation, Δa^*, resulting from a large variation, $\Delta N_0 = N_{02} - N_{01}$, of the horizontal component of the tensile force. By integrating Equation (7), after some elementary passages, it results

$$\begin{aligned} \Delta a^* = \int_{N_{01}}^{N_{02}} \frac{p^2\, a^3}{12\, N_0^3} dN_0 &= \frac{p^2\, a^3}{24}\left(\frac{1}{N_{01}^2} - \frac{1}{N_{02}^2}\right) = \frac{\gamma^2\, a^3}{24}\left(\frac{1}{\sigma_{01}^2} - \frac{1}{\sigma_{02}^2}\right) \\ &= \frac{\gamma^2\, a^3}{24}\left(\frac{\sigma_{02}^2 - \sigma_{01}^2}{\sigma_{01}^2\, \sigma_{02}^2}\right) = \frac{\gamma^2\, a^3}{24\, \sigma_{01}^3}\, \frac{1+\overline{\sigma}}{\overline{\sigma}^2} \Delta\sigma, \end{aligned} \tag{10}$$

and, consequently,

$$\frac{\Delta\sigma_0}{\Delta\varepsilon_f} = \frac{1}{E_s^*(\sigma_{01}, \sigma_{02})} = \frac{\gamma^2\, a^2}{24\, \sigma_{01}^3}\, \frac{1+\overline{\sigma}}{\overline{\sigma}^2}. \tag{11}$$

As a matter of fact, these solutions are satisfactory only when the cable highly stressed and, therefore, the cable sag is small with respect to its chord; consequently, several theoretical and numerical studies have been devoted to refine the solutions, aiming to enlarge their field of application [4–15].

Among them, particularly remarkable appear the approach adopted by Irvine [11], who introduced the characteristic parameter of a suspended cable, λ^2, including both the shape and the deformational properties of the cable. The abovementioned parameter λ^2 is defined by

$$\lambda^2 = \left(\frac{\gamma\, a}{\sigma_0}\right)^2 \frac{a\, E}{\sigma_0\, L_e}, \tag{12}$$

where L_e,

$$L_e = \int_0^a \left(\frac{ds}{dx}\right)^3 dx, \tag{13}$$

is a relevant property of the cable, usually known as virtual length.

When the chord length, a, is much bigger than the sag of the cable, d, L_e can be acceptably estimated as

$$L_e \cong a\left(1 + 8\left(\frac{d}{a}\right)^2\right). \tag{14}$$

For cable-stayed bridges, the parameter λ^2 is usually smaller than one, but for long stays it can be even bigger than three. For suspension bridges, λ^2 is usually bigger than 100 [6].

Following Irvine [11], it is possible to estimate the equivalent modulus, $E_{t,eq1}$, using the simplified expression

$$E_{t,eq1} = \frac{d\sigma}{d\varepsilon} = \frac{E}{1 + \frac{\lambda^2}{12}}. \quad (15)$$

When applicable, Equation (15) is much more precise than Equation (1), although, due to the approximations introduced in deriving it, it leads to some surprisingly bizarre results when σ_0 is small, a is great and the virtual length L_e is calculated via exact integration of Equation (13), and not applying the simplified Equation (14).

Although arriving at simple and easy to handle formulae, the application of classical methods is subject to severe restrictions, which limit their fields of application, especially for flabby cables. In fact, these approaches do not completely consider the effect of the variation of the cable configuration upon the arrangement of external loads. To allow a general application of the equivalent modulus concept, exact closed form solutions are thus necessary.

In a previous paper [16], we suggested an original method, based on the virtual work theorem, to find the equivalent tangent modulus of an inclined stay, taking into account the effect of its self-weight. Assuming a deformed catenary shape of the cable, that method allowed to derive accurate closed-form solutions describing the nonlinear behavior of the cable, in terms of equivalent tangent stiffness. Since deduced considering all relevant aspects of the problem, the formulae proposed in [16] are valid on the whole field of interest, independently on the inclination of the cable, on the stress level, on the sag of the catenary, and on the cable material, so allowing a generalized application of the equivalent stiffness approach. That method provides different expressions, depending on the nature of the relative displacement between the extremities of the cable, i.e., depending on whether both end sections are fixed, or one end section is fixed and the other can moves during the loading process; in other words, depending on whether the cable length is fixed or not during the loading process. Moreover, the solutions are so refined that, in case both cable ends are fixed, they are function of the absolute sign of the vertical component, dh, of the relative displacement between the cable ends themselves, that governs the work done by the self-weight of the cable as a result of that relative displacement. In fact, in [16] (page 1098), where $k = dh/da$ indicates the ratio between the vertical and the horizontal components of the relative displacement of the cable ends A and B, and σ the normal stress in the cable whose horizontal component is σ_0, it is remarked that: "It must also be emphasized that the apparent modulus can result larger, even significantly, than E, for example when $k{\cdot}dh > 0$ in A, because of the weight of the cable. In this case, for $\sigma \to \infty$, the curves $E_{ft,eqA} = E_{ft,eqA}(\sigma)$ and $E_{ft,eqB} = E_{ft,eqB}(\sigma)$ approach the horizontal asymptote $E_{ft,eqA} = E$ from above and from below, respectively. In addition, an in-depth examination of the formula (36.b) induces to infer that negative values of the apparent modulus at the cable end B cannot be excluded, for example when σ_0 is small and $k > 0$, and that the region where the apparent modulus is negative raises as the span increases. Negative values of the apparent modulus, clearly unacceptable in design practice, happen when increase of the chord length implies decrease of the stress at the cable end, or vice versa: this is again due to the cable weight. These results suggest resorting to a more operational definition of the equivalent modulus, in some way accounting for the weight effects described before. In fact, in the usual mechanical model the cable is replaced by a weightless straight rod, and the weight of the cable is concentrated at the ends of the equivalent rod. From now on, an improved equivalence can be established subtracting from the work done by the cable weight for the end displacement dh, the work amount associated with rigid body motion, W_{pr}, (... ...)". For a more exhaustive illustration of these relevant aspects, the interested reader can refer to [16].

More recently, several research works tackled the question [17–20], suggesting improvements of classical formulae, mainly aiming to define appropriate cable elements to be implemented in finite element models. Anyhow, as it can be easily ascertained comparing the proposed solutions with those reported in [16], all these works arrive to approximate formulae, because, in solving the problem, some parameters, especially relevant in the low stress region, are disregarded. In addition, all these

studies do not consider that the solution is also depending on the nature of the relative displacement of cable ends.

In view of the implementation of suitable elements in the finite element method, another actual research topic focuses on the influence of bending and shear stiffness on the cable behavior [21,22]. Nevertheless, as they are relevant only in peculiar situations, bending stiffness and shear stiffness can be often interpreted as local perturbations of the general solution, obtained by neglecting them.

Horizontal stays can be seen as a particular case of inclined cables, so that their equivalent axial stiffness can be derived from the general expressions given in [16], considering the cable ends at the same level, so setting to zero the difference h between their elevations. Unfortunately, these general expressions are extremely intricate and composed by many terms, most of which assume an indeterminate form for h tending to zero. Consequently, although representing in principle the simplest practical situation, application of the general formulae to horizontal stays require cumbersome calculations; moreover, the complexity of the expression contributes to confuse the influence of different parameters.

The aim of the study is to illustrate how the equations of the equivalent stiffness of horizontal stays can be deduced implementing the procedure based on the virtual work theorem, already successfully applied in the general case for inclined cables [16].

The outcomes of the procedure are new expressions of the equivalent tangent modulus of the cable, depending on the nature of the boundary conditions. As they accurately consider all influencing parameters, these rather compact innovative formulae can be again applied without restrictions.

Referring to some relevant case studies, the results obtained adopting the proposed approach are critically discussed, also in comparison with the outcomes of classical simplified methods.

2. The Bernoulli Equation of the Catenary

To facilitate the reading, in the following, the classical derivation of the Bernoulli catenary equation is shortly summarized.

As known, disregarding elastic deformations, or, equivalently, assuming $E = \infty$, the deformed shape cable of constant cross section A_0, fixed at its ends A and B, and subject to the self-weight (Figure 1), can be obtained from the equilibrium equation of a part of the cable, indicated with $[A, C]$ in Figure 2:

$$\vec{0} = \vec{R}_A + \int_0^{s'} \vec{p}(s)ds + \vec{N}(s'). \tag{16}$$

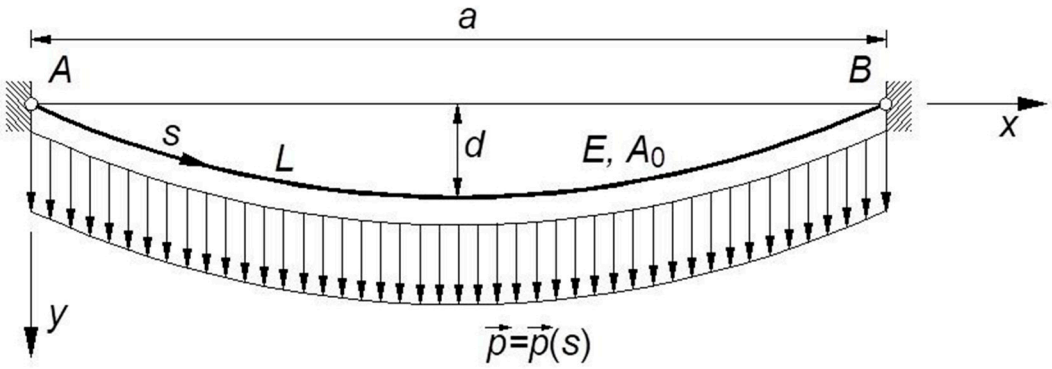

Figure 1. Deformed configuration of a horizontal cable due to self-weight.

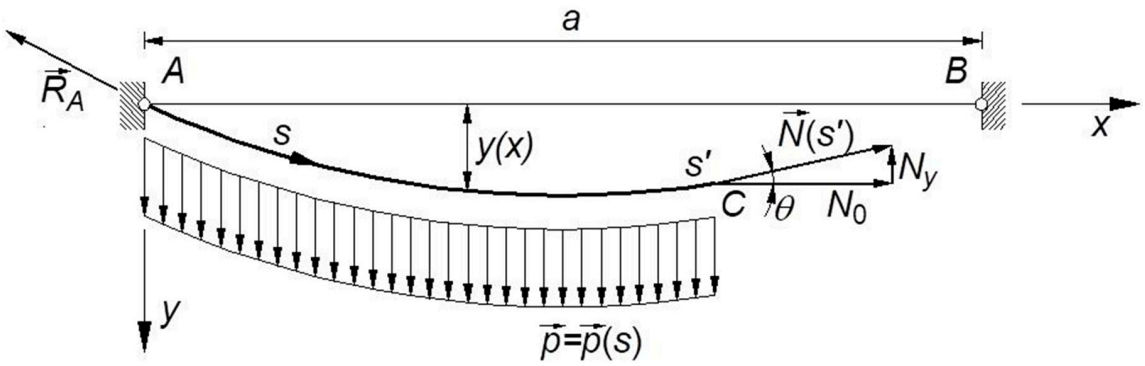

Figure 2. Loads applied on the cable part $[A, C]$.

In Equation (16) $\vec{R}_A$ is the reaction at the cable extremity A, $\vec{p}(s)$ is the self-weight of the cable per unit length, and $\vec{N}(s')$ the tensile force at the end C of the considered part of the cable.

Differentiating it with respect to s', Equation (16) becomes

$$\vec{0} = \vec{p} + \frac{d\vec{N}(s)}{ds} \tag{17}$$

thus leading, in a Cartesian coordinate system with vertical y-axis, to

$$\begin{cases} \frac{d(N\cos\theta)}{ds} = 0 \\ \frac{d(N\sin\theta)}{ds} = p \end{cases} \tag{18}$$

where $\theta = \arctan(dy/dx)$, N_0 the horizontal component of $\vec{N}$, and $y = y(x)$ the equation of the cable configuration. Obviously, since $N_0 = N\cos\theta$, N_0 is not depending on s.

Duly combining the two Equations (18) we find

$$\begin{aligned} N_0 \tfrac{d}{ds}\tan\theta = p \quad &\rightarrow \tfrac{d}{ds}\tan\theta = \tfrac{p}{N_0} \rightarrow \tfrac{dy'}{ds} = \tfrac{p}{N_0} \rightarrow \tfrac{dy'}{dx}\tfrac{dx}{ds} = \tfrac{p}{N_0} \rightarrow y'' \\ &= -\tfrac{p}{N_0}\sqrt{1+y'^2}, \end{aligned} \tag{19}$$

whose solution is the classical Bernoulli's catenary equation

$$y(x) = -\frac{N_0}{p}\cosh\left(\frac{p}{N_0}x + C_1\right) + C_2, \tag{20}$$

where the constants C_1 and C_2 depend on the boundary conditions.

Let the origin of the coordinate system be at the extremity A of the cable; considering that the length of the horizontal chord is a, and the boundary conditions are $y(0) = 0$ and $y(a) = 0$, in the current situation, Equation (20) becomes

$$y(x) = -\frac{N_0}{p}\left[\cosh\left(\frac{p}{N_0}x - \frac{p\,a}{2\,N_0}\right) - \cosh\left(-\frac{p\,a}{2\,N_0}\right)\right], \tag{21}$$

while the cable length L results

$$L = \int_0^a \sqrt{1+y'^2}dx = -\frac{N_0}{p}\int_0^a y''dx = -\int_0^a \cosh\left(\frac{p}{N_0}x - \frac{p\,a}{2\,N_0}\right)dx = 2\,\frac{N_0}{p}\sinh\left(\frac{p\,a}{2\,N_0}\right), \tag{22}$$

expressions that are given in every book of rational mechanics.

According to Irvine [11], introducing the Hooke's law for the cable, Equation (20) can be suitably modified to take into account also elastic deformations, so that inextensibility assumption is not necessary. Moreover, elastic deformations must be explicitly considered only when the solution depends on them, that is when the initial unstrained length of the cable is smaller than the chord length, and the cable requires some additional pre-strain to be installed. In all other cases, Equation (20) is still applicable, on the condition that it is expressed considering the final configuration, and the value of the unit self-weight $p(s)$ is calculated considering the length of the stretched cable.

3. The Virtual Work Theorem for the Cable

The nonlinear behavior of the cable can be studied by means of the theorem of virtual works, following the advanced method already adopted by the author in [16].

Starting from the deformed configuration of the cable, the virtual work theorem is applied considering a virtual horizontal relative displacement dx between the cable extremities, A, and B. Obviously, the resulting equation can be also derived assuming that the end A is fixed and the relative displacement is concentrated in the end B, or vice versa.

When the cable end B is shift by dx_B, in B', two significant cases can occur, depending on the actual constraint at the cable end B: in fact, the virtual displacement can affect the length of the cable, or the length of the chord. In the former case, which also reproduces the tensioning phase of a real cable, the cable itself is assumed to run over a fixed pulley in B (Figure 3): in this case, the length of the chord is not affected by the displacement dx_B, which entirely results in a variation dL of the cable length L. On the contrary, in the latter case, which represents the most frequent operational condition of a structural cable, the cable extremities are assumed fixed in A and in B: consequently, the displacement dx_B is entirely converted in a variation da of the cable chord (Figure 4).

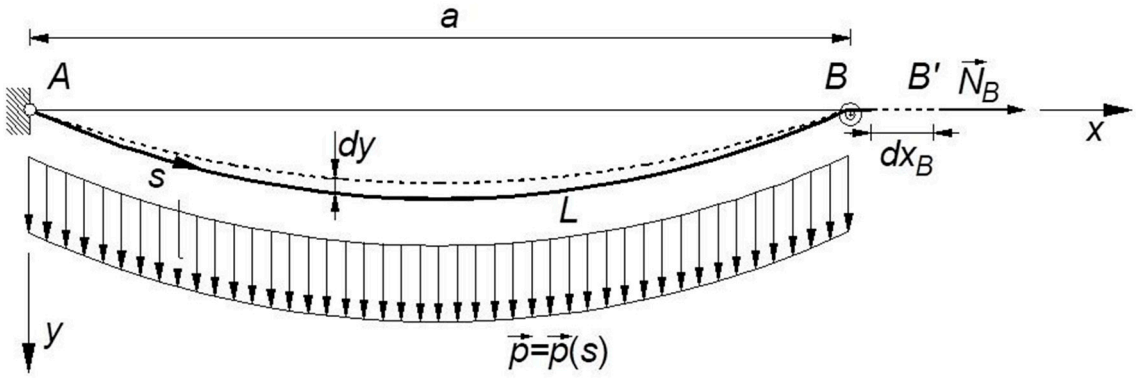

Figure 3. Cable running over a fixed pulley in B, i.e., a = const.

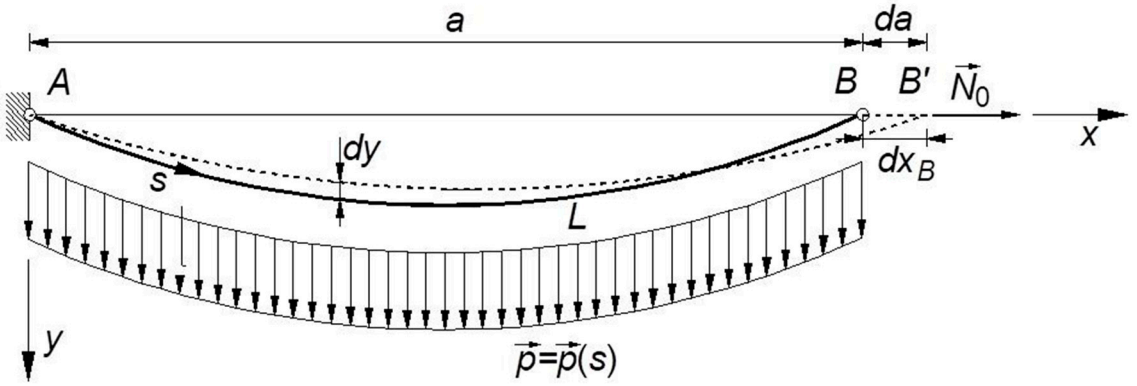

Figure 4. Cable with ends fixed in A and in B.

Recalling that the cable ordinate $y(x)$ is expressed by Equation (21), in both situations, the expression of the virtual work equation is

$$\left(\vec{N}_B + d\vec{N}_B\right)\cdot d\vec{x}_B + \int_0^L \vec{p}\cdot d\vec{y}\; ds \;=\; \int_V \sigma d\varepsilon \; dV, \tag{23}$$

where σ is the normal stress, $d\varepsilon$ the variation of the longitudinal strain, V the volume of the cable, and $d\vec{y}$ the variation of $y(x)$ caused by the modification of the shape of the cable itself.

Obviously, when the deformations of the cable are disregarded, i.e., the cable is assumed to be inextensible, the left-hand side of Equation (23) is zero.

Since $d\vec{N}_B\cdot d\vec{x}_B$ is negligible with respect to $\vec{N}_B\cdot d\vec{x}_B$, and $\vec{p}$ is parallel to $\vec{y}$, Equation (23) can be reduced to

$$\vec{N}_B\cdot d\vec{x}_B + \int_0^L p\; dy\; ds \;=\; \int_V \sigma d\varepsilon \; dV. \tag{24}$$

Let x be the abscissa of an arbitrary point of the cable, we can remark that the variation dy of the ordinate of that point is the result of the relative displacement component along the cable chord, da, as well as of the variation dN_0 of the horizontal component of the axial force. The total variation, dy, can be interpreted as the sum of two contributions: one, dy_{inex}, associated with the modification of the shape of the cable, assumed to be inextensible; the other, dy_e, due to the variation of the elastic strain produced by dN_0:

$$dy = dy_{inex} + dy_e. \tag{25}$$

The variation dy_{inex} associated with the configuration change can be obtained by differentiating Equation (25) and considering that, for a given abscissa x, $y(x)$ depends only on N_0 and on a. Consequently, dy_{inex} results:

$$dy_{inex} = \frac{\partial y}{\partial a}da + \frac{\partial y}{\partial N_0}dN_0. \tag{26}$$

Obviously, in case the chord length is fixed, i.e., a is constant, Equation (26) reduces to:

$$dy_{inex} = \frac{dy}{dN_0}dN_0. \tag{27}$$

On the other hand, the variation dy_e due to the elastic strain variation is a function of the vertical component of the axial force only. That contribution can be implicitly taken into account in the expression of the cable's equation, assuming that the length of the "inextensible" cable is equal to its final, deformed length. The variation of the cable ordinate dy_e can be easily derived recalling that, according to Irvine [11], the contribution of elastic strain variations to the final configuration of a cable, made with a linear elastic material, is

$$\Delta y_e(s) = \frac{N_0}{E\,A_0}s\; y'^{(0)} - p\frac{s^2}{2\,E\,A_0}. \tag{28}$$

In fact, differentiating Equation (28) with respect to N_0, dy_e finally results

$$dy_e = \left(\frac{y'(0)}{E\,A_0} + \frac{N_0}{E\,A_0}\frac{dy'(0)}{dN_0}\right)s\; dN_0 \tag{29}$$

It must be underlined that in the present study effects of the elastic deformations are properly considered, being disregarded, as usual, only the effect of the elastic variation of the cable length on the integration limits.

4. Equivalent Stiffness of Stays Running over a Fixed Pulley on One End

Cables running around a fixed pulley on one end are considered first (Figure 3). In that case, the chord length a is not varying, and dy_{inex} is given by Equation (27). Hypothesizing a linear elastic material, Equation (24) becomes

$$N_B\, dL + \int_0^L p \frac{dy}{dN_0} dN_0\ \ ds = \int_0^L \frac{N}{EA_0}\, dN\, ds. \tag{30}$$

Recalling Equations (19) and (29), Equation (30) converts in

$$\begin{aligned} N_0\ \sqrt{1+y'(a)^2}\, dL \quad & + \int_0^L p \tfrac{\partial y_e}{\partial N_0} ds\, dN_0 + \int_0^a p \tfrac{dy}{dN_0} dN_0 \ \ \sqrt{1+y'^2}\, dx \\ & = \tfrac{N_0\, dN_0}{EA_0} \int_0^a \left(1+y'^2\right)^{\frac{3}{2}}\ \ dx. \end{aligned} \tag{31}$$

Given that

$$\frac{dy}{dN_0} = -\frac{\cosh\left(\frac{p\,a}{2\,N_0} - \frac{p\,x}{N_0}\right)}{p} + \frac{\cosh\left(\frac{p\,a}{2\,N_0}\right)}{p} - \frac{\left(x-\frac{a}{2}\right)\sinh\left(\frac{p\,a}{2\,N_0} - \frac{p\,x}{N_0}\right)}{N_0} - \frac{a\,\sin h\left(\frac{p\,a}{2\,N_0}\right)}{2\,N_0}, \tag{32}$$

and that

$$\begin{aligned} \int_0^L p \tfrac{\partial y_e}{\partial N_0} ds \quad & = p\left(\tfrac{y'(0)}{E\,A_0} + \tfrac{N_0}{E\,A_0}\tfrac{dy'(0)}{dN_0}\right) \int_0^L s\, ds \\ & = \tfrac{p\,L^2}{2\,E\,A_0}\left(\sinh\left(\tfrac{p\,a}{2\,N_0}\right) - \tfrac{p\,a}{2\,N_0}\ \cosh\left(\tfrac{p\,a}{2\,N_0}\right)\right), \end{aligned} \tag{33}$$

Equation (31) reduces to

$$\begin{aligned} N_0 \cosh\left(\tfrac{p\,a}{2\,N_0}\right) dL \quad & + \tfrac{p\,L^2\,dN_0}{2\,E\,A_0}\left[\sinh\left(\tfrac{p\,a}{2\,N_0}\right) - \tfrac{p\,a}{2\,N_0}\ \cosh\left(\tfrac{p\,a}{2\,N_0}\right)\right] \\ & - \int_0^a \Big\{\cosh\left(\tfrac{p\,a}{2\,N_0} - \tfrac{p\,x}{N_0}\right)\left[\tfrac{p\,a}{2\,N_0}\sinh\left(\tfrac{p\,a}{2\,N_0}\right)\right. \\ & - \left(\tfrac{p\,a}{2\,N_0} - \tfrac{p\,x}{N_0}\right)\sinh\left(\tfrac{p\,a}{2\,N_0} - \tfrac{p\,x}{N_0}\right) + \cosh\left(\tfrac{p\,a}{2\,N_0} - \tfrac{p\,x}{N_0}\right) \\ & \left. - \cosh\left(\tfrac{p\,a}{2\,N_0}\right)\right]\Big\}\, dx\, dN_0 = \tfrac{N_0\,dN_0}{EA_0} \int_0^a \cosh^3\left(\tfrac{p\,a}{2\,N_0} - \tfrac{p\,x}{N_0}\right) dx, \end{aligned} \tag{34}$$

which, integrating and simplifying, leads to

$$\begin{aligned} \cosh\left(\tfrac{p\,a}{2\,N_0}\right) dL \quad & + \left[\tfrac{1}{4\,p}\ \sin h\left(\tfrac{p\,a}{N_0}\right) - \tfrac{a}{4\,N_0}\ \cos h\left(\tfrac{p\,a}{N_0}\right)\right] dN_0 \\ & = \tfrac{N_0}{6\,EA_0\,p}\left[9\ \sin h\left(\tfrac{p\,a}{2\,N_0}\right) + \ \sin h\left(\tfrac{3\,p\,a}{2\,N_0}\right)\right. \\ & \left. -24\ \sinh^3\left(\tfrac{p\,a}{2\,N_0}\right) + 6\tfrac{p\,a}{N_0}\ \sin h\left(\tfrac{p\,a}{2\,N_0}\right)\sin h\left(\tfrac{p\,a}{N_0}\right)\right] dN_0. \end{aligned} \tag{35}$$

Referring the deformation to the x axis, the apparent variation of the chord length dx_B equals the variation of the cable length dL, $dx_B = dL$, so that a kind of equivalent tangent elastic modulus, $E_{pt,eq}$, can be derived

$$\begin{aligned} \tfrac{1}{E_{pt,eq}} = \tfrac{d\varepsilon_x}{d\sigma_0} \quad & = \tfrac{1}{\cosh\left(\frac{\gamma\,a}{2\,\sigma_0}\right)}\left\{\tfrac{\sigma_0}{6\,a\,E\,\gamma}\left[9\ \sin h\left(\tfrac{\gamma\,a}{2\,\sigma_0}\right)\right.\right. \\ & + \sinh\left(\tfrac{3\,\gamma\,a}{2\,\sigma_0}\right) - 24\ \sinh^3\left(\tfrac{\gamma\,a}{2\,\sigma_0}\right) + 6\ \tfrac{\gamma\,a}{\sigma_0}\ \sin h\left(\tfrac{\gamma\,a}{2\,\sigma_0}\right)\sin h\left(\tfrac{\gamma\,a}{\sigma_0}\right)\Big] \\ & \left. - \tfrac{1}{4\,a\,\gamma}\ \sin h\left(\tfrac{\gamma\,a}{\sigma_0}\right) + \tfrac{1}{4\,\sigma_0}\ \cos h\left(\tfrac{\gamma\,a}{\sigma_0}\right)\right\} \end{aligned} \tag{36}$$

where $d\varepsilon_x$ is the apparent strain variation of the chord, σ_0 the horizontal component of the tension and γ the specific weight of the cable material:

$$d\varepsilon_x = \frac{dx_B}{a}, \sigma_0 = \frac{N_0}{A_0}, \ \gamma = \frac{p}{A_0} \tag{37}$$

5. Equivalent Stiffness of Stays Fixed at Their Ends

If the cable is fixed at its ends (Figure 4), obviously it is $dx_B = da$; therefore, by applying Equations (25), (26) and (29), dy results

$$N_0\, da + \int_0^L p \frac{\partial y_e}{\partial N_0} ds\, dN_0 + \int_0^a p\left(\frac{\partial y}{\partial N_0} dN_0 + \frac{\partial y}{\partial a} da\right) \sqrt{1 + y'^2}\, dx = \frac{N_0\, dN_0}{EA_0} \int_0^a \left(1 + y'^2\right)^{\frac{3}{2}}\, dx. \tag{38}$$

Recalling the results of the previous section, and considering that

$$\begin{aligned} \int_0^a p \frac{\partial y}{\partial a} \sqrt{1 + y'^2}\, dx\, da &= \frac{p}{2} \int_0^a \cosh\left(\tfrac{p\,a}{2\,N_0} - \tfrac{p\,x}{N_0}\right) \cosh\left(\tfrac{p\,a}{2\,N_0} - \tfrac{p\,x}{2\,N_0}\right) \sinh\left(\tfrac{p\,a}{2\,N_0}\right) dx\, da \\ &= N_0 \sinh^2\left(\tfrac{p\,a}{2\,N_0}\right) da, \end{aligned} \tag{39}$$

Equation (24) assumes the form

$$\begin{aligned} \cosh^2\left(\tfrac{p\,a}{2\,N_0}\right) dL &+ \left[\tfrac{1}{4\,p} \sin h\left(\tfrac{p\,a}{N_0}\right) - \tfrac{a}{4\,N_0} \cos h\left(\tfrac{p\,a}{N_0}\right)\right] dN_0 \\ &= \tfrac{N_0}{6\,EA_0\,p}\Big[9 \sin h\left(\tfrac{p\,a}{2\,N_0}\right) + \sin h\left(\tfrac{3\,p\,a}{2\,N_0}\right) \\ &\quad -24 \sinh^3\left(\tfrac{p\,a}{2\,N_0}\right) + 6 \tfrac{p\,a}{N_0} \sin h\left(\tfrac{p\,a}{2\,N_0}\right) \sin h\left(\tfrac{p\,a}{N_0}\right)\Big] dN_0, \end{aligned} \tag{40}$$

from which one derives

$$\begin{aligned} \frac{1}{E_{ft,eq}} = \frac{d\varepsilon_x}{d\sigma_0} &= \frac{1}{\cosh^2\left(\frac{\gamma\,a}{2\,\sigma_0}\right)} \Big\{ \tfrac{\sigma_0}{6\,a\,E\,\gamma} \Big[9 \sin h\left(\tfrac{\gamma\,a}{2\,\sigma_0}\right) \\ &\quad + \sinh\left(\tfrac{3\,\gamma\,a}{2\,\sigma_0}\right) - 24 \sinh^3\left(\tfrac{\gamma\,a}{2\,\sigma_0}\right) + 6\, \tfrac{\gamma\,a}{\sigma_0} \sin h\left(\tfrac{\gamma\,a}{2\,\sigma_0}\right) \sin h\left(\tfrac{\gamma\,a}{\sigma_0}\right)\Big] \\ &\quad - \tfrac{1}{4\,a\,\gamma} \sin h\left(\tfrac{\gamma\,a}{\sigma_0}\right) + \tfrac{1}{4\,\sigma_0} \cos h\left(\tfrac{\gamma\,a}{\sigma_0}\right) \Big\}. \end{aligned} \tag{41}$$

A comparison of Equation (41) with Equation (36) demonstrates that the equivalent along the chord stiffness of the cable fixed at its ends is always bigger than the equivalent stiffness of the cable, having the same characteristics, running over a pulley. In fact, as $\gamma a/\sigma_0 > 0$, the ratio ω between $E_{ft,eq}$ and $E_{pt,eq}$ is always bigger than one:

$$\omega = \frac{E_{ft,eq}}{E_{pt,eq}} = \cosh\left(\frac{\gamma\,a}{2\,\sigma_0}\right) > 1. \tag{42}$$

Evidently, it is

$$\lim_{\sigma_0 \to \infty} \omega = 1, \tag{43}$$

therefore, confirming that the cable behavior tends to be independent on the end conditions for "flat" and highly stressed cables.

The dependence of ω on the product γa and on the horizontal component of the normal stress, σ_0, is illustrated in Figure 5, where curves are parameterized according the value of the horizontal stress component σ_0.

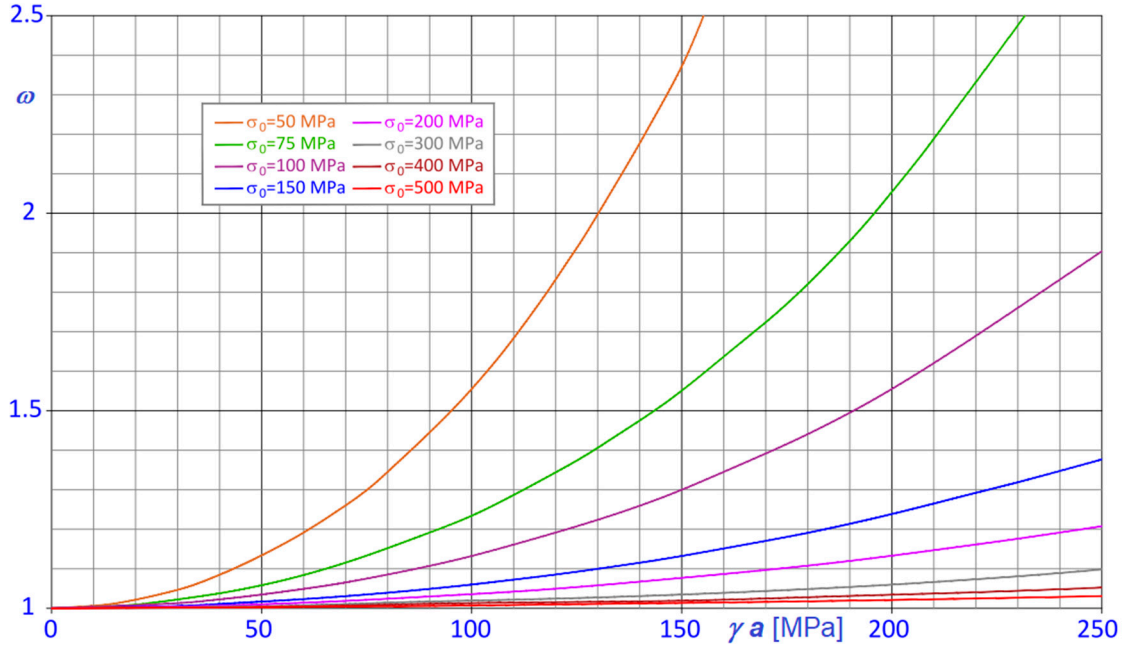

Figure 5. $\omega - \gamma a$ curves parameterized in terms of horizontal stress component σ_0.

In the diagram, considering that $\sigma_0 > 500$ MPa implies $\omega \approx 1$, values of σ_0 have been selected in the range 50–500 MPa. More generally, it can be remarked that ω differs significantly from one only when the stress level is low or γa is high. To exemplify, considering a steel cable having a chord length a = 1000 m, for which γa = 78.5 MPa, it results $\omega < 1.1$, provided that the horizontal stress component satisfies the inequality $\sigma_0 > 88.5$ MPa.

It must be emphasized that expressions (36) and (41) are much more relevant than one might assume at first sight. In fact, once assigned the initial stress, nonlinear constitutive equations $\sigma_0 = \sigma_0(\varepsilon_x)$, pertaining to the equivalent spring or truss element, can be accurately derived via numerical integration of Equations (36) and (41), taking into account also the chord length variation, if required.

6. Some Relevant Examples

To highlight the refinements achieved by using the proposed approach, the new formula (41) has been applied to evaluate the apparent stiffness $E_{ft,eq}$ in the relevant case of steel cables, considering chord lengths varying in the range 10–3000 m. According to usual design assumptions, the following values have been adopted for the specific weight and the elastic modulus of the steel cable: $\gamma = 78.5$ kN/m^3; $E = 1.8 \times 10^5$ MPa, thus obtaining the results summarized in Figures 6 and 7.

In Figure 6, the $E_{ft,eq} = E_{ft,eq}(\sigma_0)$ curves are parameterized in terms of the chord length, a; conversely, in Figure 7, $E_{ft,eq} = E_{ft,eq}(a)$ curves are parameterized in terms of the horizontal component of the tension, σ_0.

Inspection of the diagrams confirms that, when the stress σ_0 is low and the chord length a is large, the equivalent modulus $E_{ft,eq}$ can be significantly smaller than E. Obviously, the effect is further intensified when the cable is running around a fixed pulley.

To facilitate the interpretation of the results, given the chord length a, it is useful to associate the value of the stress component σ_0 with the corresponding cable sag, d, or, better, with the corresponding sag to chord ratio k, given by

$$k = \frac{d}{a} = \frac{\sigma_0}{a\,\gamma}\left(\cosh\left(\frac{\gamma\, a}{2\,\sigma_0}\right) - 1\right) \tag{44}$$

as illustrated in the bi-logarithmic graph of Figure 8. In Figure 8, curves have been derived considering that, in practice, upper limits exist for the cable sag d, for example, due to the limited height of the

pylons or to the limited elevation of the cable attachments over the roof, over the deck, or over the valley floor. For that reason, in the considered examples, it has been assumed $d \leq 500$ m, implying that $k - \sigma_0$ curves are limited on the right and that σ_0 is bounded from below.

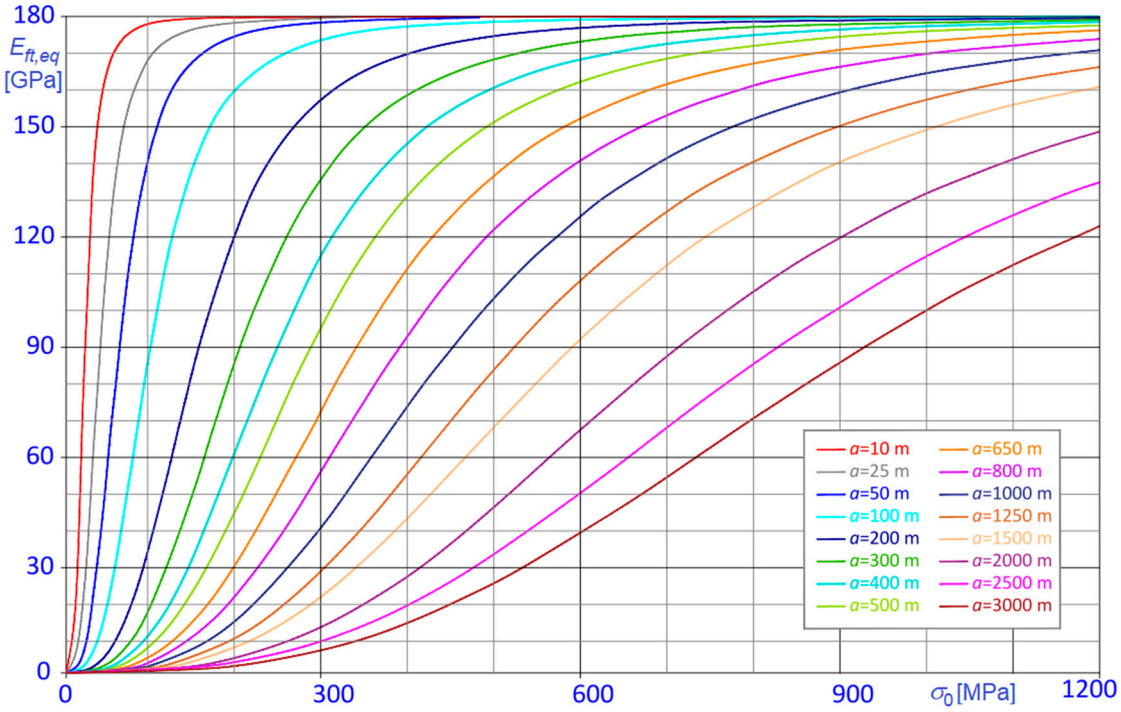

Figure 6. $E_{ft,eq} - \sigma_0$ curves parameterized in terms of chord length, a.

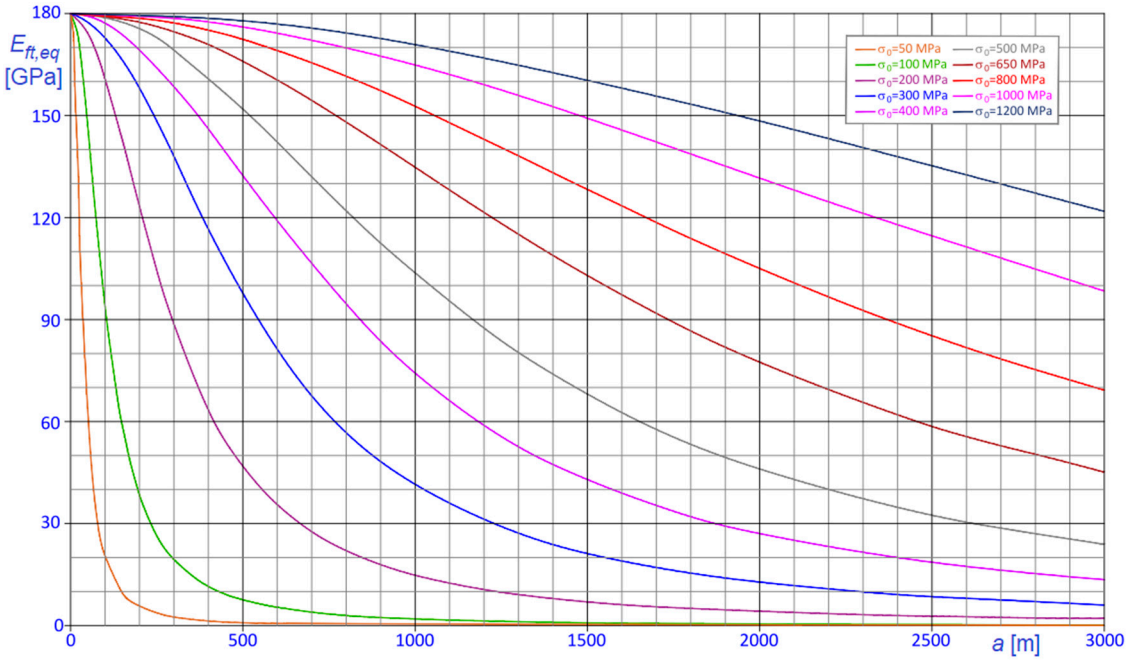

Figure 7. $E_{ft,eq} - a$ curves parameterized in terms of horizontal stress component, σ_0.

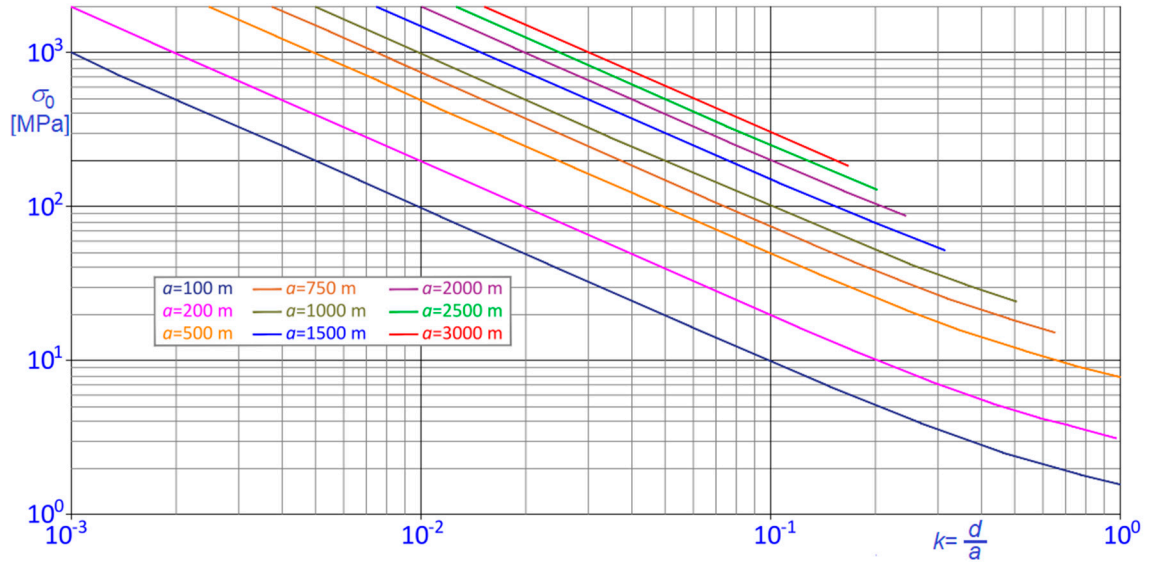

Figure 8. $\sigma_0 - k$ curves for steel cables, parameterized in terms of chord length, a.

For instance, in the present case, where $\gamma = 78.5$ kN/m^3, and $d \leq 500$ m, the lower limit of σ_0, which is about 50 MPa when $a = 1500$ m, increases to about 85 MPa when $a = 2000$ m, to finally attain values around 130 MPa and 180 MPa for $a = 2500$ m and $a = 3000$ m, respectively. Clearly, when cables are made with materials other than steel, lower limits of σ_0 vary, depending on the specific weight, γ, of the cable material itself.

To check the capability of the classical Dischinger's formula to predict the effective behavior of steel cables, the ratios $E_{t,eq}/E_{ft,eq}$ between the Dischinger modulus, $E_{t,eq}$ (Equation (1)), and that predicted with the proposed formula, $E_{ft,eq}$ (Equation (41), are plotted against the chord length a and the horizontal stress component σ_0 in Figures 9 and 10, respectively. Curves are consequently parameterized in terms of σ_0 in Figure 9 and in terms of a in Figure 10.

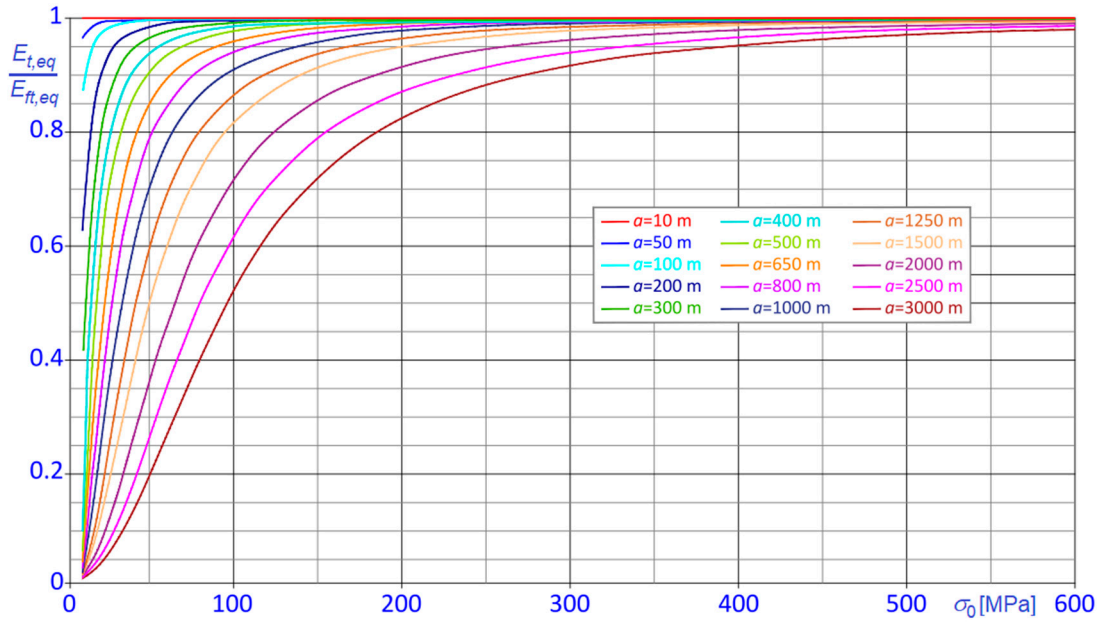

Figure 9. $\frac{E_{t,eq}}{E_{ft,eq}} - \sigma_0$ curves for steel cables, parameterized in terms of a.

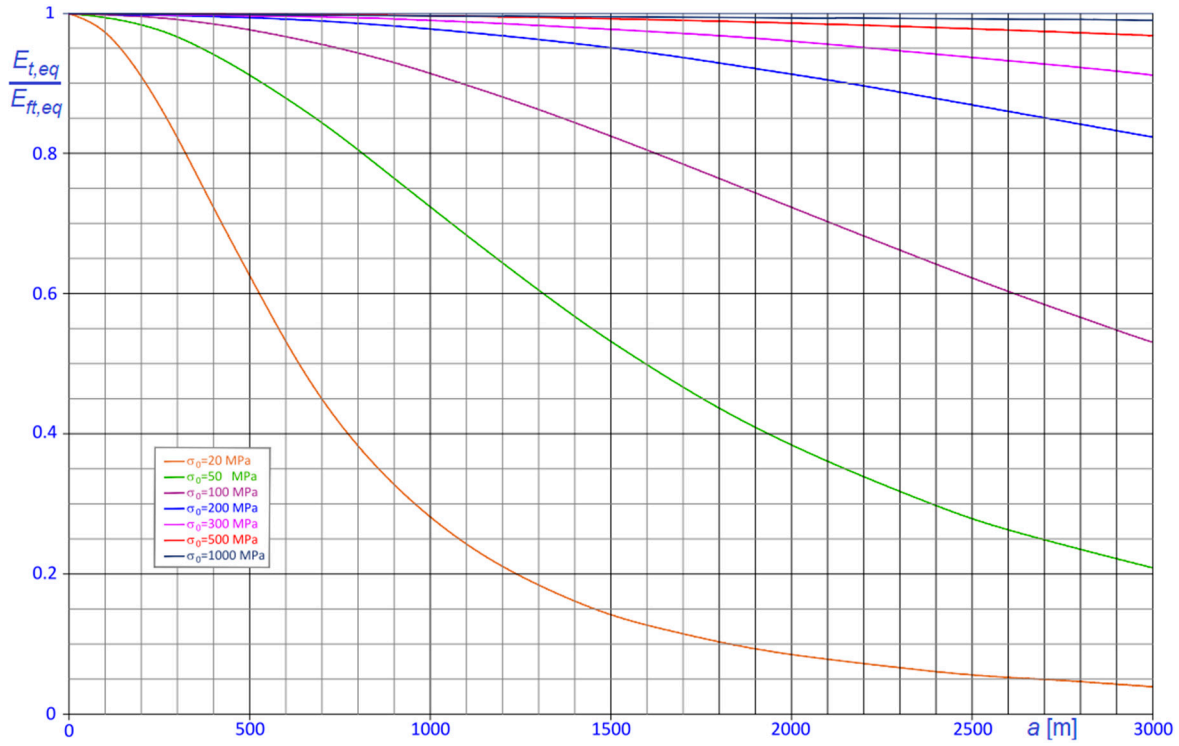

Figure 10. $\frac{E_{t,eq}}{E_{ft,eq}} - a$ curves for steel cables, parameterized in terms of σ_0.

The diagrams demonstrate that the equivalent stiffness derived via the classical Dischinger's formula is regularly lower than the one derived with the formulation proposed here and that the error increases as soon as the stress in the cable decreases, or, evenly, the sag to chord ratio, k, increases.

7. Generalization of the Results

Thus far, the results for the steel cables have been discussed. Despite its relevance, this is not the unique significant case that can be met in different fields of current design practice, where the use of many other traditional or innovative structural materials can be more suitable.

A discussion about the applications of these materials is outside the scope of the study, even if cables made with innovative structural materials are increasingly proposed not only for cable-stayed and suspension bridges [23,24], but also for general structural applications [25,26], as well as in the framework of strengthening, restoration and repair interventions [27]. Further studies consider hybrid solutions too [28].

It is known that the efficiency of cables made by different materials can be efficiently compared through two particularly relevant properties: the specific strength, f_t/ρ, which is the ratio between the tensile strength f_t and the density ρ of the cable material, and the specific stiffness, E/ρ which is the ratio between the elastic modulus and the density of the cable material.

For the steel cables, usually it is $f_t \approx 1770$ MPa and $E \approx 180$ MPa, so that $f_t/\rho \approx 22.5$ kNm/kg and $E/\rho \approx 22.9$ MNm/kg, while cables made by more modern and advanced materials, like aramid, liquid crystal aromatic polyester (LCP), polybenzoxazole (PBO) or carbon fibers, exhibit more favorable values. Some reference values for mechanical properties of cables made by different artificial, metallic, or biologic materials are reported in Table 1.

Table 1. Reference values of relevant mechanical properties of various cable materials.

Cable Material	Density ρ $[kg/m^3]$	Elastic Modulus E	Ultimate Strength f_t [MPa]	Specific Stiffness E/ρ [MNm/kg]	Specific Strength f_t/ρ [kNm/kg]
Aramid fiber (high modulus)	1440	112	3000	77.8	208
Aramid fiber (normal modulus)	1440	70.5	2900	49.0	201
Liquid crystal aromatic polyester (LCP) fiber	1410	66	2830	46.8	201
Polybenzoxazole (PBO) fiber	1560	270	3950	173	253
Carbon fiber	1560	170	2500	109	160
Steel strand	7850	180	1770	22.9	22.5
Steel wire	7850	206	1900	26.2	24.2
Copper	8940	110	240	12.3	2.68
Aluminum	2700	69	105	25.5	3.89
Nylon fiber	1140	4.56	610	4.0	53.5
Polyester fiber	1380	13.8	790	10.0	57.2
Cotton rope	1540	7.9	225	5.1	14.6
Hemp rope	1490	32	300	21.5	20.1
Flax rope	1540	27	340	17.5	22.1
Jute rope	1500	25.8	230	17.2	15.3
Abaca (Manila hemp) rope	1320	30	300	22.7	22.7
Sisal	1320	30	250	22.7	18.9
Silk (silkworm)	1320	10	650	7.6	49.2
Silk (spider)	1100	12	900	10.9	81.8

The specific stiffness is related to the magnitude of nonlinear effects on cable behavior. In fact, Equation (39) suggests that, for a given value of σ_0, k reduces as γ increases, so that, generally, as higher is the value of the specific stiffness as smaller are the nonlinear effects.

But that conclusion is correct only when the comparison refers to materials with significantly different densities and with comparable elastic moduli, like, for example, steel and PBO or steel and carbon fiber. To better clarify this remark, the $E_{ft,eq}/E - \sigma_0$ curves, pertaining to cables made by different materials, namely, steel, carbon fiber, PBO and nylon, are compared in Figure 11, considering two different chord lengths, $a = 100$ m and $a = 1000$ m.

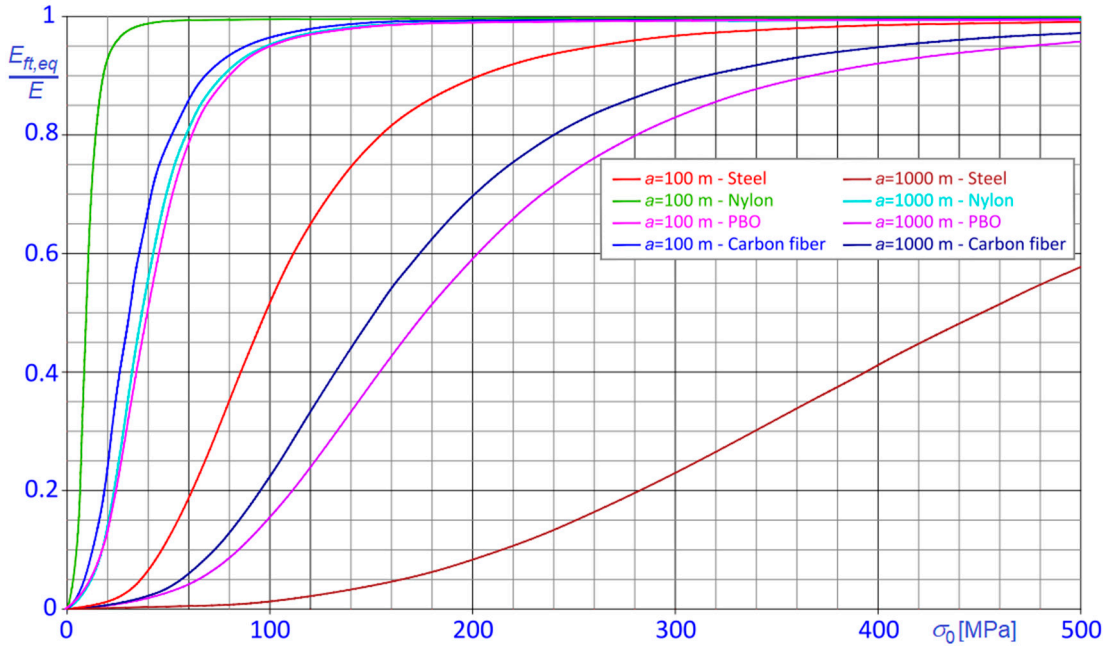

Figure 11. $\frac{E_{t,eq}}{E} - \sigma_0$ curves for steel, carbon fiber, PBO and nylon cables: $a = 100$ m; $a = 1000$ m.

Truly, looking at the curves in Figure 11, much more articulated and interesting conclusions can be derived about the dependence of the ratio $E_{ft,eq}/E$ on the specific stiffness. In fact, considering two cables made with different materials, nonlinear effects are more pronounced in that characterized by bigger specific stiffness only if the densities of the materials are comparable, or the elastic moduli of the materials are considerably different, as it is evident comparing the curves pertaining to of PBO, carbon fiber and nylon cables, or those pertaining to steel and nylon cables in Figure 11.

That behavior can be explained considering that nonlinear effects are mainly determined by the work made by the self-weight of the cable (see Equation (24)). Once the cable configuration is fixed, the work of the self-weight turns out almost independent on the elastic modulus of the material, so that its influence on $E_{ft,eq}/E$ is more relevant for materials characterized by smaller modulus, E.

On the other hand, some additional conclusions can be also derived regarding the dependence of the ratio $E_{ft,eq}/E$ on the ratio $\sigma_0/(\gamma\, a)$, as a function of the cable material.

Recalling Equation (30), it is clear that cables made of different materials, and having the same sag and the same chord length, are associated to the same ratios $\sigma_0/(\gamma\, a)$, or σ_0/γ.

In Figure 12, the $E_{ft,eq}/E - \sigma_0/\gamma$ curves for steel, carbon fiber, PBO and nylon cables are diagrammatically shown considering again two different chord lengths, $a = 100$ m and $a = 1000$ m.

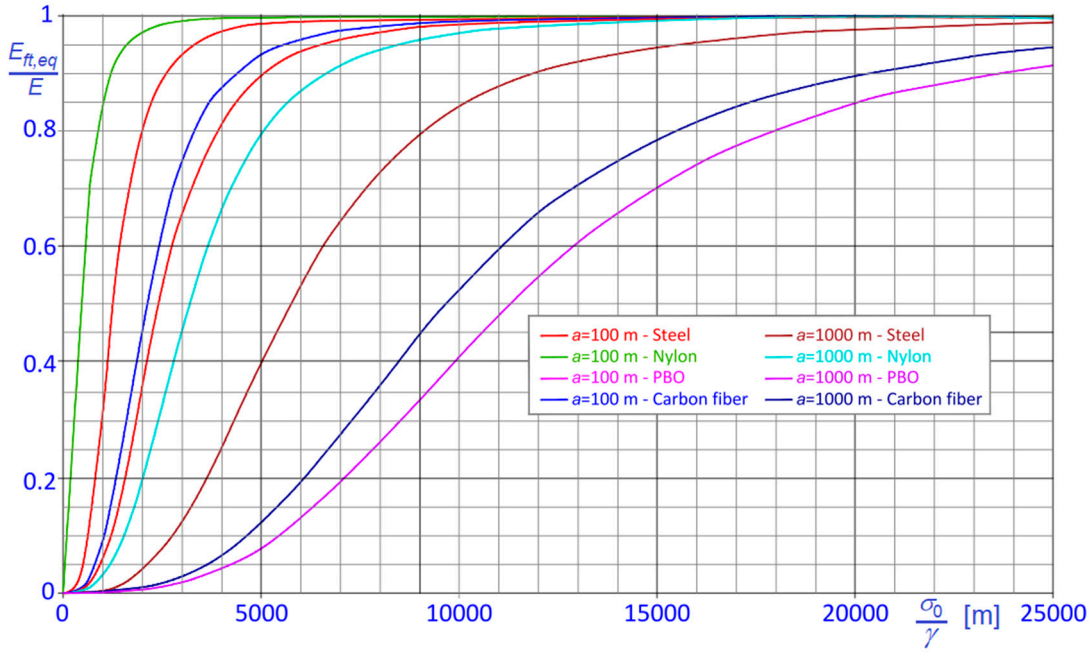

Figure 12. $\frac{E_{t,eq}}{E} - \frac{\sigma_0}{\gamma}$ curves for steel, carbon fiber, PBO and nylon cables: $a = 100$ m; $a = 1000$ m.

From the diagram in Figure 12, it is evident that, among the considered materials, PBO cables are characterized by the lowest $E_{ft,eq}/E$ ratio, while nylon cables are characterized by the highest $E_{ft,eq}/E$ ratio, and that $E_{ft,eq}/E$ ratio is bigger for steel cables than for carbon fiber cables. Therefore, it is again confirmed that the magnitude of nonlinear effects increases with the specific stiffness of the material only when materials with sensibly different densities and similar elastic moduli are compared; on the contrary, as stated before, comparing materials with similar densities leads to exactly the opposite conclusion.

It must be stressed that the comparisons discussed above are devoted to point out the effects of the variation of elastic modulus and density of various materials on the extent of nonlinear behavior of the cable, independently on the mechanical or economic feasibility of the solutions which are envisaged here. For additional information, see, for example, [23].

We underline that the proposed formulae maintain their validity also when long term effects are significant, like for creep-sensitive materials, provided that the pertinent time dependent creep

coefficient is known [29], and that the Young modulus of the material is replaced with the appropriate age-adjusted effective elastic modulus.

8. Conclusions

The nonlinear behavior of horizontal cables under the self-weight is the subject of a number of studies, often aiming to find suitable expressions for the equivalent along the chord stiffness.

The topic is very relevant in view of practical applications, as the results allow important simplifications of nonlinear analysis of cable structures. For example, in finite element analysis (FEA), replacing the cables or parts of them with suitable equivalent nonlinear spring or truss elements considerably increase the speed and the efficiency of the analysis. On the other hand, the knowledge of the equivalent stiffness can be a robust practical tool to rapidly check results of nonlinear FEA.

Several simplified formulae have been proposed over the years, starting from the classical expression proposed by Dischinger, still frequently used in current design practice, and arriving to much more refined solutions, like that due to Irvine.

In a previous study, starting from the classical Bernoulli equation of the catenary, and applying the virtual work theorem, accurate and general expressions of the along the chord tangent stiffness of inclined cables subject to the self-weight were derived, as a function the nature of the relative displacement of the cable extremities. Depending on the boundary conditions of the stay, two relevant situations can occur, corresponding to distinct solutions: in fact, it could happen that both ends of the cable are attached, like in normal working conditions, so that the unstrained length of the cable is fixed; or, alternatively, that one end is fixed and the other is running around a fixed pulley, like in the cable tensioning phase, when the unstrained length of the cable varies as a function of the applied tensile force. The study demonstrates that the equivalent stiffness of the cable in the former case is bigger than in the latter. It must be underlined that not only classical simplified formulae, but also more refined approaches proposed over the years, are unable to make such a fine distinction, depending on the restraints at the stay ends.

The abovementioned innovative general closed form solutions, suitable to be used in modeling equivalent spring or truss elements, are also valid for horizontal cables, but they are so complex and the calculations so complicated, that their reduction to that particular case was not easy.

For that reason, the above-recalled method has been applied to directly deduce the equations of the equivalent stiffness of horizontal stays.

The outcomes of the procedure are new expressions of the equivalent tangent modulus of the horizontal cable, depending on the nature of the boundary conditions. As they accurately consider all influencing parameters, these rather compact innovative formulae can be again applied without restrictions, independently on the inclination of the cable, on the sag of the catenary, and on the cable material, thus allowing a generalized application of the equivalent stiffness approach, in particular in the low stress region. Of course, the formulae given here for horizontal cables, which can be also applied for slightly inclined cables, coincide with those derived from the expressions for inclined cables when h tends to zero.

A relevant case study, involving horizontal steel stays with fixed ends, and chord length a varying in the range $10 - 3000$ m, is discussed in detail, also aiming to estimate the approximations inherent with the Dischinger's approach. The outcome is that Dischinger's formula underestimates the actual stiffness of the cable, especially when the value of the horizontal component of the stress σ_0 is small.

Results have been extended to other significant cases, taking into account various natural or artificial cable materials, so highlighting that the magnitude of nonlinear effects in the cable depends not only on the specific stiffness, but also on the elastic modulus and on the density of the material.

Long terms effects can be also taken into account, provided that the elastic modulus of the material is replaced with the pertinent age-adjusted effective modulus.

Moreover, in case the cable is inhomogeneous, there are relevant situations where the proposed formulae can be applied without modifications, like in case of a hybrid cable; or in case the cable

is obtained connecting two or more stretches made of different materials, on condition that specific weight and elastic modulus of distinct stretches are comparable, but, evidently, the latter case seems quite unrealistic.

Depending on the particular structure under consideration, other relevant cases can be envisaged in the practice: for example, in cable-stayed bridges or in other guyed structures, where the main distributed load acting on the stay is mainly the self-weight of the stay itself, the reference configuration to be considered for the cables s the catenary; while, in suspension bridges or in other structures characterized by horizontal and inclined cables sustaining uniformly distributed loads, the reference configuration to be considered for the cable is the parabola.

The proposed solutions for horizontal stays, together with the general expressions already found for inclined stays, provide a complete and original set of formulae for the evaluation of the equivalent stiffness of stays.

Evidently, according to an approach frequently adopted in the existing studies, it is possible to use these expressions also in case of loaded cables, suitably increasing the unit self-weight of the cable in order to simulate the presence of the uniformly distributed load, i.e., fitting the actual deformed parabolic shape, with the appropriate catenary.

Although reasonable for taut cables, that approximation becomes unacceptable as soon as the cable sag increases, and the parabola significantly deviates from the catenary. Further studies will be thus addressed to natural improvements of the proposed approach, aiming to arrive to general solutions also for uniformly loaded cables, hypothesizing parabolic deformed configurations.

In addition, other promising extensions can be also envisaged, aiming to encompass, when relevant, the bending stiffness, and the shear stiffness of the cable as well.

Funding: This research received no external funding.

Conflicts of Interest: The authors declare no conflict of interest.

References

1. Dischinger, F. Hängebrücken für schwertse Verkehrslasten, I. *Bauingenieur* **1949**, *24*, 65–75. (In German)
2. Dischinger, F. Hängebrücken für schwertse Verkehrslasten, II. *Bauingenieur* **1949**, *24*, 107–113. (In German)
3. Ernst, J.H. Der E-modul von Seilen under Berücksichtigung des Durchhanges. *Bauingenieur* **1965**, *40*, 52–55. (In German)
4. Como, A.; Grimaldi, A.; Maceri, F. Statical behaviour of long-span cable-stayed bridges. *Int. J. Solids Struct.* **1985**, *21*, 831–850. [CrossRef]
5. Daniell, W.E.; Macdonald, J.H.G. Improved finite element modeling of a cable-stayed bridge through systematic manual tuning. *Eng. Struct.* **2007**, *29*, 358–371. [CrossRef]
6. de Sá Caetano, E. *Cable Vibrations in Cable-Stayed Bridges*; IABSE: Zürich, Switzerland, 2007.
7. Fleming, J.F. Nonlinear static analysis of cable-stayed bridge structures. *Comp. Struct.* **1979**, *10*, 621–635. [CrossRef]
8. Freire, A.M.S.; Negrão, J.H.O.; Lopes, A.V. Geometrical nonlinearities on the static analysis of highly flexible steel cable-stayed bridges. *Comp. Struct.* **2006**, *84*, 2082–2140. [CrossRef]
9. Gimsing, N.J. *Cable Supported Bridges: Concept and Design*, 2nd ed.; J. Wiley & Sons: New York, NY, USA, 1997.
10. Hajdin, N.; Michaltsos, G.T.; Konstantakopulus, T.G. About the equivalent elastic modulus of elasticity of cables of cable-stayed bridges. *Facta Univ. Niš Univ.* **1998**, *1*, 569–575.
11. Irvine, H.M. *Cable Structures*; MIT Press: Cambridge, MA, USA, 1992.
12. Li-zhong, W.; Zhen, G.; Feng, Y. Quasi-static three-dimensional analysis of suction anchor mooring system. *Ocean Eng.* **2010**, *37*, 1127–1138. [CrossRef]
13. Pao-Hsii, W.; Hung-Ta, L.; Tzu-Yang, T. Study on nonlinear analysis of a highly redundant cable-stayed bridge. *Comp. Struct.* **2002**, *80*, 165–182.
14. Troitsky, M.S. *Cable Stayed Bridges: Theory and Design*, 2nd ed.; BSP Professional Books: Oxford, UK, 1988.
15. Tschemmernegg, F.; Obholzer, A. Einfach abgespannte Seile bei Schrägseilbrücken. *Bauingenieur* **1981**, *56*, 325–330. (in German).

16. Croce, P. Non-linear behavior of heavy stays. *Int. J. Solids Struct.* **2013**, *50*, 1093–1107. [CrossRef]
17. Crusells-Girona, M.; Filippou, F.C.; Taylor, R.L. A mixed formulation for nonlinear analysis of cable structures. *Comp. Struct.* **2017**, *186*, 50–61. [CrossRef]
18. Li, C.; He, J.; Zang, Z.; Liu, Y.; Ke, H.; Dong, C.; Li, H. An improved analytical algorithm on main cable system of suspension bridge. *Appl. Sci.* **2018**, *8*, 1358. [CrossRef]
19. Tan, H.; Zeng, Y.; Zhang, X. Cable spring effect and its longitudinal restraint stiffness on towers. *Proc. ICE Bridge Eng.* **2020**, *173*, 78–85. [CrossRef]
20. Bertrand, C.; Acary, V.; Lamarque, C.-H.; Ture Savadkoohi, A. A robust and efficient numerical finite element method for cables. *Int. J. Num. Methods Eng.* **2020**, *121*, 4157–4186. [CrossRef]
21. Hussein, H.; Gouttefarde, M.; Pierrot, F. Static modeling of Sagging Cables with flexural rigidity and shear forces. In *Advances in Robot Kinematics 2018*; Lenarcic, J., Parenti-Castelli, V., Eds.; Springer International Publishing: Cham, Switzerland, 2019; pp. 310–318. [CrossRef]
22. Zhang, Y.; Wang, J.; Ye, G.; Xu, R. Bending stiffness of parallel wire cables including interfacial slips among wires. *ASCE J. Struct. Eng.* **2018**, *144*, 04018164. [CrossRef]
23. Zhang, X. Mechanics feasibility of using CFRP cables in super long-span cable-stayed bridges. *Struct. Eng. Mech.* **2008**, *29*, 567–579. [CrossRef]
24. Xiong, W.; Cai, C.S.; Xiao, C. The use of carbon fiber-reinforced polymer (CFRP) composites for cable-stayed bridges. In *Advanced Composites in Bridge Construction and Repair*; Kim, J.L., Ed.; Woodhead Publishing: Cambridge, UK, 2017; pp. 210–264. [CrossRef]
25. Meier, U. Carbon fiber reinforced polymer cables: Why? Why Not? What If? *Arab J. Sci. Eng.* **2012**, *37*, 399–411. [CrossRef]
26. Liu, Y.; Zwingmann, B.; Schlaich, M. Carbon fiber reinforced polymer for cable structures—A Review. *Polymers* **2015**, *7*, 2078–2099. [CrossRef]
27. Micelli, A.; Cascardi, A.; Marsano, M. Seismic strengthening of a theatre masonry building by using active FRP wires. In *Proc. of the 16th Int. Brick and Block Masonry Conf. IBMAC 2016 Brick and Block Masonry—Trends, Innovations and Challenges, Padova, IT, June 2016*; Modena, C., da Porto, F., Valluzzi, M.R., Eds.; CRC Press/Balkema: Leiden, NL, USA, 2016; pp. 753–761.
28. Cai, H.; Aref, A.J. On the design and optimization of hybrid carbon fiber reinforced polymer-steel cable system for cable-stayed bridges. *Compos. Part B Eng.* **2015**, *68*, 146–152. [CrossRef]
29. Yang, D.; Zhang, J.; Song, S.; Zhou, F.; Wang, C. Experimental investigation on the creep property of carbon fiber reinforced polymer tendons under high stress levels. *Materials* **2018**, *11*, 2273. [CrossRef] [PubMed]